Stripes, Zigzags, and Slow Dynamics in Buckled Hard Spheres

Yair Shokef* and Tom C. Lubensky

Department of Physics and Astronomy, University of Pennsylvania, Philadelphia, Pennsylvania 19104, USA

(Received 30 July 2008; published 29 January 2009)

We study the analogy between buckled colloidal monolayers and the triangular-lattice Ising antiferromagnet. We calculate free-volume-induced Ising interactions, show how lattice deformations favor zigzag stripes that partially remove the Ising model ground-state degeneracy, and identify the martensitic mechanism prohibiting perfect stripes. Slowly inflating the spheres yields jamming as well as logarithmically slow relaxation reminiscent of the glassy dynamics observed experimentally.

DOI: 10.1103/PhysRevLett.102.048303 PACS numbers: 82.70.Dd, 75.10.Hk, 75.50.Ee, 81.30.Kf

Geometric frustration, manifested, for example, in the triangular-lattice antiferromagnetic (AFM) Ising model [1], occurs whenever local interaction energies cannot be simultaneously minimized. It gives rise to highly degenerate ground states, unusual phases of matter [2], and possibly slow or glassy dynamics [3], whose properties even after decades of research are not fully understood. Here we present a theoretical study of a colloidal system, one of a class of artificial frustrated systems in which the state of each constituent can be directly visualized [4], that provides new insight into the microstructure of frustrated systems and its connection with their dynamics.

We study hard spheres confined between parallel plates. For plate separation slightly greater than the sphere diameter and at sufficiently high sphere density, the spheres buckle upward or downward [5–7] from their lower-density positions on a hexagonal lattice. This buckling gives rise to a choice of two states for each sphere, analogous to the two states of Ising model spins [5,8]. The tendency of spheres to maximize free volume introduces an effective repulsive interaction that favors configurations with neighboring spheres in opposite states just as the AFM Ising interaction favors opposite states of neighboring spins. As in the triangular-lattice AFM Ising model, frustration arises because it is impossible to arrange the three particles on any triangular plaquette such that all pairs of neighbors are in opposite states. In the AFM Ising model on a rigid lattice, there is an extensive number of ground-state configurations (implying an extensive ground-state entropy) in which neighboring spins on two of the three bonds on each plaquette are in opposite states. Given this analogy between our colloidal system and the AFM Ising model, it is reasonable to conjecture that the colloidal system might exhibit ground-state degeneracies and dynamics similar to those of the rigid-lattice AFM Ising model. Recent experiments in diameter-tunable-microgel systems revealed subextensive ground-state entropy and glassy dynamics [9]. Our theoretical study will address the differences between the colloidal system and the rigid-lattice Ising model and make some conjectures about a likely closer analogy between the colloidal system and the AFM Ising model on a compressible lattice [10].

We show that the short-ranged AFM behavior in this hard-sphere system may be explained by a simple geometrical model relating it to the nearest-neighbor Ising model. However, the out-of-plane buckling induces local in-plane lattice distortions that, as in the elastic Ising model, partially remove the Ising ground-state degeneracy and select configurations with zigzagging stripes of up and down spheres. This ''ground state'' lacks the local zero-energy modes found in the Ising model on a rigid triangular lattice, and as a result, the colloidal system exhibits dynamics qualitatively slower than those of the Ising model. Moreover, stripes require global deformations incompatible with the system's boundary conditions and consequently break up into a martensite [11] and form a new partially disordered and highly degenerate ''ground state.''

The free energy of our hard-sphere system is dictated by its phase-space volume, which is a collective function of all the particles in the system; hence this system is not exactly equivalent to an Ising model with pairwise additive interactions. Nonetheless, we may compare our system to the nearest-neighbor Ising model on the triangular lattice and ask what is the strength of AFM interactions that best describes our system.

A ''microscopic'' state is specified by the positions $\{x_i, y_i, z_i\}$ of all particles $1 \le i \le N$. We coarse grain these states into Ising-like configurations specified by $\{s_i\}$ with $s_i = \mathrm{sign}(z_i)$ (x, y are the coordinates in the plane of the confining walls, z is perpendicular to the walls, and $z = 0$ is at the middle of the cell). The probability of a particular configuration $\{s_i\}$ of hard spheres is equal to the $3N$-dimensional integral $V(\{s_i\})$ over all states belonging to that configuration, divided by the total phase-space volume V_{tot} of all configurations: $P_{\mathrm{HS}}(\{s_i\}) = V(\{s_i\})/V_{\mathrm{tot}}$. We would like to equate this to the probability of finding the corresponding configuration in the Ising model, $P_I(\{s_i\}) = \exp(\beta J \sum s_i s_j)/Z$, where $\beta = 1/k_B T$ is the inverse temperature, J is the interaction strength, the sum runs over all nearest-neighbor pairs, and Z is the canonical partition function.

Unlike the commonly used cell model, which approximates the phase-space volume of a system as a product of single-particle free volumes, our model equates P_{HS} and P_I

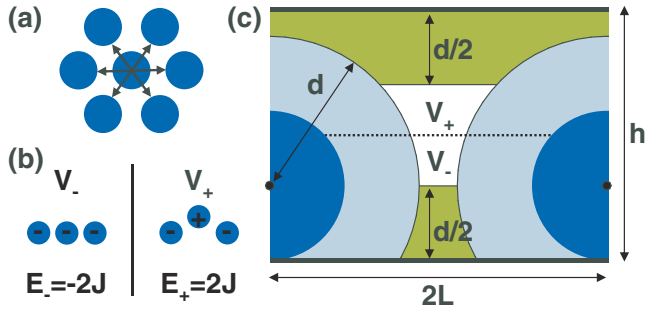

FIG. 1 (color online). Free-volume model. (a) Top view. Free volume originates from motion along axes to each of the neighbors. (b) Side view. Up particle surrounded by down particles has more free volume (lower energy) than a down particle. (c) Surrounding neighbors touch wall and are separated by $2L$; central particle is confined to the vertical plane. Large circles are volumes excluded by neighbors, horizontal bands are volumes excluded by the walls, remaining white region is the central particle's free volume, divided at the middle of the cell height (dotted line) into V_+ and V_-.

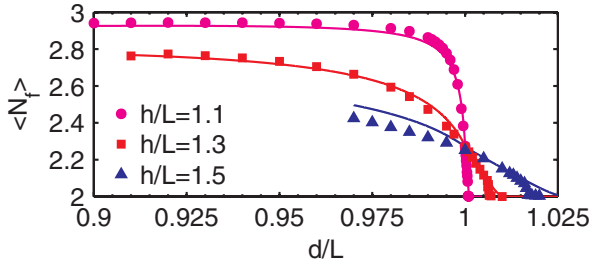

FIG. 2 (color online). Average number of frustrated bonds per particle vs sphere diameter and cell height. Free-volume model (lines) agrees with Monte Carlo simulations (symbols).

by assuming that $V(\{s_i\})$ is a product of contributions from all nearest-neighbor "bonds": $V(\{s_i\}) = \prod v(s_i s_j; h, d, L)$, where the pair contribution v depends on $s_i s_j$ and on the wall separation h, the sphere diameter d, and the in-plane number density, which we characterize by the spacing L of the underlying triangular lattice. We evaluate $v(s_i s_j)$ in a quasi-one-dimensional approximation by allowing particles i and j to move only in the vertical plane passing through the axis connecting their lattice positions [see Fig. 1(a)]. We consider a particle, which we call the central particle, and its two neighbors along one of the principal lattice directions [see Fig. 1(b)]. If the two neighbors are in opposite Ising states, the free volumes resulting from the central one being up or down are equal by symmetry. When the two neighbors are in the same state (down, without loss of generality), the central particle has more free volume (V_+) when it is up than when it is down (V_-). We calculate V_+ and V_- from the geometrical setting of Fig. 1(c) and equate the ratio of the probabilities of finding the two configurations in Fig. 1(b) for hard spheres to that of the Ising model: $V_+/V_- = \exp(-\beta E_+)/\exp(-\beta E_-) = \exp(-4\beta J)$. From this, we deduce that the hard-sphere system corresponds to an Ising model with an effective AFM interaction, $\beta J_{\text{eff}}(d, h, L) = -\ln(V_+/V_-)/4 < 0$.

For given geometrical parameters d, h, L, we evaluate V_+ and V_- and determine the effective interaction strength βJ_{eff}. We then use the exact solution of the Ising model [1] to calculate the average number $\langle N_f \rangle$ of frustrated neighbors per particle (we refer to $s_i s_j = -1$ as satisfied and to $s_i s_j = 1$ as frustrated), which provides a measure of short-range AFM order. $\langle N_f \rangle = 2$ is the value in the ground state, and $\langle N_f \rangle = 3$ corresponds to a random configuration. Figure 2 shows the agreement between our simple model and three-dimensional Monte Carlo (MC) simulations. Simulations included $N = 1600$ spheres with steps consisting of small displacements of single spheres as well as area-preserving box deformations, in which the angle or aspect ratio of the simulated parallelogram was allowed to change [7]. To probe cases with $d > L$, we start with striped configurations that can accommodate the maximal sphere diameter by lattice deformation (see below), wait 4×10^5 steps, and then average $\langle N_f \rangle$ over additional 4×10^5 steps. We plot results only of cases for which d was large enough for the system to have long-range sixfold orientational order $\Psi_6 \equiv \langle \exp(i6\theta_{jk}) \rangle > 0.5$ (θ_{jk} is the angle the bond between j and k forms with an arbitrary axis, and the average is over all nearest-neighbors pairs [12]). Small spheres ($d < L$) in a wide cell ($h/L = 1.5$) are weakly confined, and the approximation that the surrounding spheres in Fig. 1(c) touch the walls fails, giving rise to small differences between the model and simulations.

For large spheres ($d > L$), simulations remain jammed in striped configurations and do not increase the value of $\langle N_f \rangle$ beyond the initial value of 2, even though they are expected to do so from the free-volume considerations incorporated in the model. To further explore this jamming, we conducted MC simulations that started at a disordered configuration with $d_0 = L$ and then ordered as the sphere diameter was gradually increased to some larger value d. The spheres were initially on a triangular lattice in the xy plane with each sphere randomly touching either the top or bottom wall. To speed simulations, we considered random jumps from touching one wall to touching the other, while keeping the xy displacements continuous. During the swelling process, once every MC step, the diameter of all spheres was increased to the maximal value allowable without overlaps. Figure 3 shows results of simulations with wall separation $h/L = 1.3$. For $d/L = 1.005$, the free-volume model predicts $\langle N_f \rangle = 2.12$, and the simulation indeed slowly equilibrates to that value by $\sim 10^5$ MC steps. For $d/L = 1.01$, the system's relaxation to the value of $\langle N_f \rangle = 2$ predicted by the model includes a logarithmically slow decay to $\langle N_f \rangle \approx 2.1$ over a time scale of 10^7 MC steps, followed by a sharp jump to the equilibrium state. For $d/L = 1.015$, although the system is expected to be at a state with $\langle N_f \rangle = 2$, it gets jammed during the swelling process at a state with $\langle N_f \rangle = 2.35$ and does not leave it over the time scales investigated here. Note that in Fig. 3

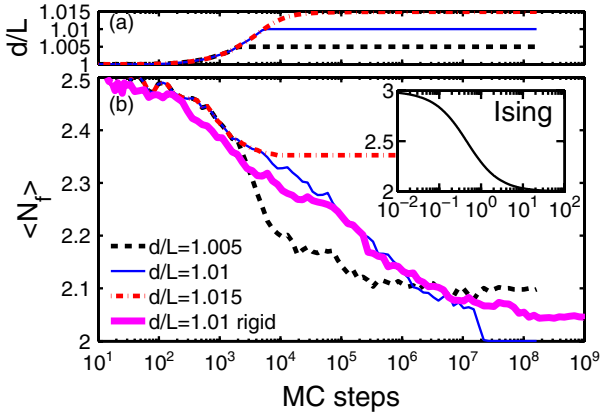

FIG. 3 (color online). (a) Sphere diameter and (b) average number of frustrated bonds per particle following swelling to different sphere diameters. Normalized cell height $h/L = 1.3$. Inset: same for Ising model following quench to $T = 0$.

we plot a single realization for each case; however, we observed similar behavior when repeating the simulations with multiple realizations. Neither jamming nor logarithmically slow relaxation occurs in the Ising model even when quenched to zero temperature (see inset).

Densely packed spheres exhibit slower dynamics than low-temperature Ising spins on a rigid lattice because the morphology of the maximally packed hard-sphere configurations differs from that of the Ising ground state. Unlike the highly disordered Ising ground state [1], the hard-sphere ''ground state'' consists of parallel zigzag stripes [Fig. 4(a)]. In the Ising model, each triangular plaquette has one bond frustrated and two satisfied. Although one-third of the bonds in the system are frustrated, and the average number of frustrated neighbors per particle is $\langle N_f \rangle = 2$, not all particles have exactly two frustrated neighbors. By considering the six triangles surrounding a certain spin in the lattice, Fig. 5(a) shows the five possible ways (up to rotations and spin inversions) to align them such that each triangle will have a single frustrated bond. The central spin may have $N_f = 0$, 1, 2, or 3 frustrated neighbors. This leads not only to disorder but also to fast relaxation dynamics since spins with $N_f = 3$ are free to flip without an energetic cost. For close-packed buckled spheres, each triplet of spheres in contact defines an equilateral triangle with sides d. As in the Ising model, one of the three spheres is up (or down) and two are down (or up), thus tilting this equilateral triangle with respect to the horizontal plane. When projected onto the plane, the tilted equilateral triangle is deformed to an isosceles triangle with one long side d along the frustrated bond and two shorter sides $x = \sqrt{d^2 - (h-d)^2} < d$ along the satisfied bonds. Each of these isosceles triangles has two small angles $\alpha = \cos^{-1}(\frac{d}{2x}) < \frac{\pi}{3}$ and a large angle $\beta = \pi - 2\alpha > \frac{\pi}{3}$. Now, close-packed configurations for the buckled spheres are equivalent to tiling the plane with these isosceles triangles. To completely cover the plane, the angles of the six triangles meeting at each vertex must sum to 2π. Figure 5(b) demonstrates that for $N_f = 0$, 1, 3 the angles sum to $6\beta > 2\pi$, $2\alpha + 4\beta > 2\pi$, and $6\alpha < 2\pi$, respectively, and thus that the triangles cannot fit together; for the two configurations with $N_f = 2$ the angles sum to $4\alpha + 2\beta = 2\pi$, enabling a perfect tiling corresponding to the maximal-density close-packed state.

The slow dynamics observed for large sphere diameters result from the lower degeneracy of these zigzagged stripe configurations compared to the Ising ground state. More importantly, the close-packed states with $N_f \equiv 2$ do not have the free particles with $N_f = 3$ that are crucial for the low-temperature dynamics in the Ising model [13]. Here, many spheres need to cooperatively rearrange in order for the system to find configurations that maximize the free volume. Spheres swollen to a very large diameter ($d/L = 1.015$ here) hardly move vertically to change their Ising configuration because the neighboring spheres do not have enough room to rearrange in the horizontal directions and to accommodate the lattice deformations required to achieve optimal packing.

When the spheres swell slowly enough, they find a configuration that maximizes free volume by each sphere having exactly two frustrated neighbors. Such configurations consist of parallel zigzagging stripes [Fig. 4(a)]. Stripes run only along two of the three principal lattice directions; hence the local distortions are nonisotropic and

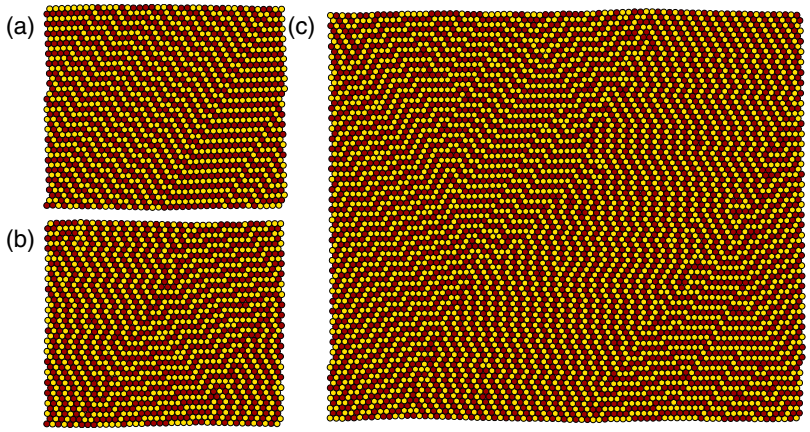

FIG. 4 (color online). Final configurations following swelling to $d/L = 1.01$ at $h/L = 1.3$. (a) Deformable box. (b and c) Rigid box. The system has $N = 1600$ (a and b), 6400 (c) spheres. Spheres touching top (bottom) wall are dark (bright). Simulation boxes are deformed parallelograms with periodic boundary conditions. For ease of presentation we copy the simulated region and plot a rectangular region of the periodic system.

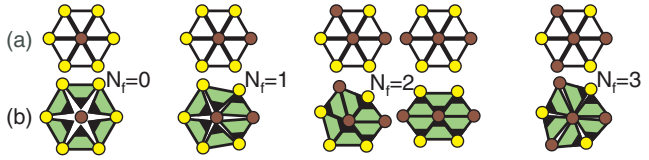

FIG. 5 (color online). Tiling with (a) equilateral triangles for the Ising ground state and (b) isosceles triangles for close-packed buckled hard spheres. The large angle β is blackened.

require a macroscopic deformation of the system. This is possible in the simulations described above in which the shape of the simulation's bounding box changes dynamically [7]. However, experimentally the spheres form crystalline domains separated by grain boundaries [12], which may be better described theoretically by rigid boundary conditions. Then, the local tendency for zigzag stripes is incompatible with the rigid boundary conditions. The tiling rules for the isosceles triangles induce local deformations along two of the three principal lattice directions, and for the system to be globally isotropic it must break up into domains with stripes running along different directions. We suspect that this is the mechanism leading to the broken stripes seen experimentally [9], and we indeed observed such martensitic states [11] when repeating the swelling simulations without allowing the simulation box to deform [14]. For instance, the case of $h/L = 1.3$, $d/L = 1.01$ relaxes in the deformable box simulations to the zigzagged striped state with $N_f \equiv 2$, whereas in a rigid box the average number of frustrated neighbors relaxes to $\langle N_f \rangle = 2.05$ [Fig. 3(b)], and the final configuration [Fig. 4(b)] consists of broken stripes. We saw similar structures [Fig. 4(c)] and relaxation to the same value of $\langle N_f \rangle$ for $N = 100$, 400, 1600, 6400. It would be interesting to test whether the size of these domains scales as the square root of the system size, as was found in other martensites [11], and whether subsequently $\langle N_f \rangle$ slowly goes to 2 in the large-N limit.

The maximal sphere diameter in a zigzag configuration is equal to that of straight stripes, and the free-volume-cell approximation does not distinguish between the two $N_f = 2$ configurations corresponding to a straight segment of a stripe and to a bend in the stripes. However, simulations and experiments seem to indicate a possible preference for straight stripes over zigzags. It is unclear if the observed zigzag patterns represent equivalence between straight and zigzagged stripes, or whether the system falls into zigzagged configurations due to kinetic reasons. It would be interesting to go beyond the mean-field description, as was done when comparing the face-centered cubic and the random hexagonal-close-packed structure of hard spheres in three dimensions [15].

The relief of frustration by lattice deformation resembles the elastic Ising model [10], which when analyzed exactly at the microscopic level yields by our isosceles tiling scheme a zigzag-stripe ground state. It would be interesting to further investigate the finite temperature behavior of that model, as well as other models with zigzag-stripe ground states [16].

We thank Yilong Han, Matt Lohr, Arjun Yodh, and Peter Yunker for involving us in their experimental study, and Bulbul Chakraborty, Randy Kamien, Andrea Liu, Carl Modes, Yehuda Snir, and Anton Souslov for helpful discussions. This work is supported by NSF MRSEC Grant No. DMR-0520020.

*Present Address: Physics of Complex Systems, Weizmann Institute of Science, Rehovot 76100, Israel.

[1] G. H. Wannier, Phys. Rev. **79**, 357 (1950); Phys. Rev. B **7**, 5017 (1973); R. M. F. Houtappel, Physica (Amsterdam) **16**, 391 (1950); **16**, 425 (1950).
[2] R. Moessner and A. R. Ramirez, Phys. Today **59**, No. 2, 24 (2006).
[3] G. Tarjus, S. A. Kivelson, Z. Nussinov, and P. Viot, J. Phys. Condens. Matter **17**, R1143 (2005).
[4] D. Davidović *et al.*, Phys. Rev. Lett. **76**, 815 (1996); Phys. Rev. B **55**, 6518 (1997); H. Hilgenkamp *et al.*, Nature (London) **422**, 50 (2003); R. F. Wang *et al.*, Nature (London) **439**, 303 (2006); Y. Qi, T. Brintlinger, and J. Cumings, Phys. Rev. B **77**, 094418 (2008); A. Libál, C. Reichhardt, and C. J. Olson Reichhardt, Phys. Rev. Lett. **97**, 228302 (2006).
[5] P. Pieranski, L. Strzelecki, and B. Pansu, Phys. Rev. Lett. **50**, 900 (1983).
[6] B. Pansu, Pi. Pieranski, and Pa. Pieranski, J. Phys. (Paris) **45**, 331 (1984); D. H. Van Winkle and C. A. Murray, Phys. Rev. A **34**, 562 (1986); T. Chou and D. R. Nelson, Phys. Rev. E **48**, 4611 (1993); P. Melby *et al.*, J. Phys. Condens. Matter **17**, S2689 (2005); N. Osterman, D. Babič, I. Poberaj, J. Dobnikar, and P. Ziherl, Phys. Rev. Lett. **99**, 248301 (2007).
[7] M. Schmidt and H. Löwen, Phys. Rev. Lett. **76**, 4552 (1996); Phys. Rev. E **55**, 7228 (1997); R. Zangi and S. A. Rice, Phys. Rev. E **58**, 7529 (1998); **61**, 660 (2000).
[8] T. Ogawa, J. Phys. Soc. Jpn. Suppl. **52**, 167 (1983).
[9] Y. Han *et al.*, Nature (London) **456**, 898 (2008).
[10] Z. Y. Chen and M. Kardar, J. Phys. C **19**, 6825 (1986); L. Gu, B. Chakraborty, P. L. Garrido, M. Phani, and J. L. Lebowitz, Phys. Rev. B **53**, 11 985 (1996).
[11] K. Bhattacharya, *Microstructure of Matersite* (Oxford University Press, New York, 2003).
[12] Y. Han, N. Y. Ha, A. M. Alsayed, and A. G. Yodh, Phys. Rev. E **77**, 041406 (2008).
[13] E. Kim, B. Kim, and S. J. Lee, Phys. Rev. E **68**, 066127 (2003).
[14] Our equilateral-to-isosceles case differs from the square-to-triangle martensitic transition in J. A. Weiss, D. W. Oxtoby, D. G. Grier, and C. A. Murray, J. Chem. Phys. **103**, 1180 (1995).
[15] W. G. Rudd, Z. W. Salsburg, A. P. Yu, and F. H. Stillinger, J. Chem. Phys. **49**, 4857 (1968); P. N. Pusey *et al.*, Phys. Rev. Lett. **63**, 2753 (1989); S. C. Mau and D. A. Huse, Phys. Rev. E **59**, 4396 (1999); C. Radin and L. Sadun, Phys. Rev. Lett. **94**, 015502 (2005); H. Koch, C. Radin, and L. Sadun, Phys. Rev. E **72**, 016708 (2005).
[16] Z. Nussinov, Phys. Rev. B **69**, 014208 (2004).